Research Square

Preprints are preliminary reports that have not undergone peer review.
They should not be considered conclusive, used to inform clinical practice,
or referenced by the media as validated information.

Synthesis and Performance Evaluation of Perfluorobutylsulfonyl Ampholytic Surfactants

Zhang Han
Sichuan Shenhe New Materials Technology Co., Ltd
Liangjun Du
Sichuan Shenhe New Materials Technology Co., Ltd
Lin Bo
Sichuan Shenhe New Materials Technology Co., Ltd
Xiangyang Yan
Sichuan Shenhe New Materials Technology Co., Ltd
Xiaojiang Li
Chongqing University of Science and Technology
Zhenfu Jia
2010007@equst.edu.cn

Sichuan Shenhe New Materials Technology Co., Ltd

Research Article

Keywords: Surfactants, surface activity, salt tolerance, amphoteric ions, short-chain perfluorinated compounds

Posted Date: July 6th, 2026

DOI: https://doi.org/10.21203/rs.3.rs-9989926/v1

License: This work is licensed under a Creative Commons Attribution 4.0 International License.
Read Full License

Additional Declarations: No competing interests reported.

Abstract

In environments characterized by extreme salinity within reservoirs, conventional surfactants often demonstrate limited salt tolerance and suboptimal performance. This study seeks to overcome the challenge of inadequate salt resistance in surfactants and enhance production efficiency in highly mineralized reservoirs through the design and synthesis of perfluorobutylsulfonyl-type amphoteric surfactants. The amphoteric salt-tolerant fluorinated surfactant FNC was synthesized via a three-step process utilizing perfluorobutylsulfonyl fluoride, N,N'-dimethyl-1,3-propanediamine, 5-chloro-1-pentene, and 3-chloropropionic acid as starting materials, with synthesis parameters optimized at each stage. Structural characterization was conducted employing infrared (IR) spectroscopy, proton nuclear magnetic resonance (^{1}H-NMR), and fluorine nuclear magnetic resonance (^{19}F-NMR) techniques. Experimental findings indicated maximum yields of 73.28%, 86.45%, and 72.88% for FNC and its intermediates FNA and FNB, respectively. The critical micelle concentration (CMC) of FNC was determined to be 6×10^{-2} g/L. Assessment of FNC's salt tolerance revealed not only exceptional resistance to high salinity but also pronounced surface activity; notably, surface tension decreased with increasing mineralization levels. The minimum surface tension recorded was 21.62 mN/m at a sodium chloride concentration of 2×10^5 mg/L and an FNC concentration of 0.3 wt%.

1. Introduction

Oil and gas, as the world's predominant energy sources and critical strategic assets, play a fundamental role in driving economic and social development. Nevertheless, with societal progress, the demand for oil and gas has escalated significantly, while global reserves are concurrently diminishing. Addressing the challenge of satisfying this increasing demand necessitates enhancing the recovery rates of existing reserves, which represents a crucial strategy for meeting future resource needs [1]. In recent years, the exploitation of coalbed methane (CBM) resources has advanced, leading to the depletion of shallow CBM reserves and shifting the focus of exploration and development toward deeper CBM deposits [2]. However, the extraction of deep CBM presents substantially greater challenges compared to shallow reserves, primarily due to the harsh conditions characterized by high mineralization levels, which impose significant difficulties on the performance of fracturing fluids [3]. Elevated salinity levels can induce surfactant precipitation, diminish surface activity, and even result in the complete loss of foam stability, thereby severely impairing the efficacy of fracturing fluids and the overall effectiveness of reservoir stimulation. Conventional surfactants have proven inadequate to meet these demanding production conditions [4]. Consequently, salt-tolerant surfactants, particularly amphoteric surfactants such as sulfobetaine, have garnered considerable research interest owing to their superior long-term stability and surface activity under high-salinity environments [5].

In comparison to anionic, cationic, and nonionic surfactants, amphoteric surfactants present several notable advantages. Firstly, they demonstrate remarkable resistance to salinity, temperature variations, and hard water conditions, maintaining a stable molecular structure that renders them well-suited for the

extreme environments encountered in deep oil, gas, and coalbed methane reservoirs, which are characterized by high salinity and elevated temperatures[6]. Secondly, amphoteric surfactants exhibit excellent compatibility, allowing them to be blended seamlessly with the other three surfactant types to achieve synergistic effects, thereby serving as essential components in oilfield surfactant formulations[7]. Thirdly, their low adsorption affinity for rock surfaces minimizes chemical loss, enhances utilization efficiency, and reduces operational costs[8]. Fourthly, these surfactants enable flexible bidirectional modulation of reservoir wettability, accommodating various rock types and thereby improving the efficacy of reservoir modification[9]. Fifthly, amphoteric surfactants possess a broad pH tolerance, making them adaptable to a wide range of field conditions[10]. Lastly, they exhibit superior foaming and foam-stabilizing capabilities, which make them particularly advantageous for foam applications in high-salinity environments. When contrasted with the limitations of anionic surfactants (notably low salt tolerance), cationic surfactants (characterized by high adsorption and poor salt tolerance), and nonionic surfactants (which suffer from low thermal stability and inadequate foaming properties), amphoteric surfactants integrate multiple beneficial attributes[11]. Consequently, they represent the most promising class of functional surfactants for application in the extraction of deep unconventional oil and gas resources.

Fluorinated surfactants are considered the ultimate "super surfactants" among all surfactants. These substances contain fluorocarbon alkyl chains in their molecular structure, which allow them to lower the surface tension of water much more effectively than their hydrocarbon counterparts. When every hydrogen atom in the alkyl chain is replaced by fluorine atoms, the compound displays unique physical and chemical characteristics.

From a molecular structural standpoint, the atomic radius of fluorine exceeds that of hydrogen, allowing fluorine atoms to more effectively encapsulate the carbon atom and serve as a protective shield. This encapsulation increases the bond energy of the carbon-carbon bonds, thereby enhancing the overall structural stability. Additionally, fluorine is the smallest atom after hydrogen and possesses a low dipole moment, which contributes to a short carbon-fluorine bond length and high bond energy. These characteristics confer resistance to molecular chain cleavage, further improving structural integrity and imparting notable thermal stability[12].

Moreover, due to the low polarizability of fluorine atoms, fluorocarbon alkyl chains exhibit reduced polarity compared to hydrocarbon chains, which translates into superior surface activity. Fluorocarbon alkyl chains also possess exceptionally low surface energy[13], resulting in pronounced hydrophobic and oleophobic properties. Consequently, fluorocarbon alkyl chains demonstrate enhanced surfactant activity relative to hydrocarbon chains. Empirical studies have shown that the surface activity of fluorocarbon surfactants is approximately 1.5 times greater than that of surfactants with alkyl chains of equivalent length[14].

Therefore, fluorinated surfactants not only exhibit superior thermal stability and salt resistance but also possess enhanced surface activity. These attributes contribute to improved post-fracturing flowback efficiency and reduced contamination within reservoirs.

Fluorocarbon chains possess notable advantages, including exceptional stability and pronounced surface activity; however, excessively long fluorocarbon chains tend to exhibit diminished solubility, thereby constraining their practical utility. Moreover, the pronounced stability of long, linear fluorocarbon chain compounds impedes their degradation in natural environments, resulting in concerns such as bioaccumulation and heightened toxicity. In response to these issues, international regulatory frameworks have long mandated the gradual elimination and prohibition of long-chain fluorocarbon surfactants with carbon chain lengths satisfying $C_nF_{2n} \geq 6$[15–17]. Conversely, fluorocarbon chains of insufficient length demonstrate reduced surface activity.

In light of these considerations, and with the dual objectives of adhering to environmental regulations and preserving surface activity, we have synthesized a novel amphoteric fluorinated surfactant tailored for application in oil and gas field extraction, specifically addressing the challenge of salt resistance. This study contributes valuable insights toward the design and development of environmentally benign, highly salt-tolerant fluorinated surfactants.

2. Materials and methods

2.1. Materials

triethylamine(purity ≥ 99.5%), dichloromethane(purity ≥ 99.5%), perfluorobut-ylsulfonyl fluoride(purity ≥ 98%), 5-chloro-1-penten(purity ≥ 98%), acetonitrile(pu-rity ≥ 99.5%), 3-chloropropionic acid(purity ≥ 98%), sodium chloride(purity ≥ 99.5%), calcium chloride(purity ≥ 99.5%), N, N'-dimethyl-1, 3-propanediamine(purit-y ≥ 98%) were procured from Shanghai McLean Biochemical Technology Co., Ltd. (Shanghai,China).

2.2. Synthesis of Perfluorobutylsulfonyl Ampholytic Surfactant (FNC)

(a) Dissolve 50 mmol of N,N'-dimethyl-1,3-propanediamine and 56 mmol of triethylamine in 120 mL of dichloromethane. Place the mixture in a 0°C water bath and stir until homogeneous. Then, slowly add 50 mmol of perfluorobutylsulfonyl fluoride dropwise. After the addition is complete, raise the temperature to 15°C and continue stirring for approximately 4 h. Once the reaction is complete, filter and dry the product to obtain the white powder intermediate FNA with an 86.45% yield.
(b) Dissolve 50 mmol of FNA and 50 mmol of 5-chloro-1-pentene in 120 mL of acetonitrile. Place the mixture in a magnetic stirrer oil bath at 80°C and reflux for 18 h. Upon completion of the reaction, distill under reduced pressure and dry to obtain the white crystalline powder intermediate FNB with an 72.88% yield.

(c) Dissolve 30 mmol of FNB, 30 mmol of 3-chloropropionic acid, and 36 mmol of triethylamine in 120 mL of acetonitrile. Place the mixture in a magnetic stirrer oil bath at 80°C and reflux for 20 h. Upon completion of the reaction, perform vacuum distillation and dry the residue to obtain the white pasty solid FNC with an 73.28% yield. The synthetic route for FNC is shown in Fig. 1.

2.3. Measurements and characterization

2.3.1. Fourier transform infrared (FTIR) analysis

Using the KBr pellet method, FNC was analyzed with a Tensor-27 infrared spectrometer (Germany) with a scanning range of 400 cm^{-1} to 4000 cm^{-1}. The test was repeated three times, and no significant differences were observed in the positions or intensities of the absorption peaks.

2.3.2. Nuclear Magnetic Resonance (^{1}H-NMR, ^{19}F-NMR) analysis

Dissolve an appropriate amount of FNC in a deuterated solvent to achieve a concentration of approximately 5 mg/mL. After complete dissolution, transfer the solution to a 5-mm diameter NMR tube and perform ^{1}H-NMR and ^{19}F-NMR measurements using an ECZ400S/L1 (Japan) liquid NMR spectrometer. The measurements were conducted at room temperature. The test was repeated three times, and no significant differences were observed in the positions or intensities of the absorption peaks.

2.3.3. Critical micelle concentration (CMC)

FNC was dissolved in deionized water to prepare solutions of various concentrations (0.01%, 0.02%, 0.03%, 0.04%, 0.05%, 0.06%, 0.07%, 0.08%, 0.09%, 0.1%, 0.2%, and 0.3%). The surface tension of these solutions at different concentrations was measured at 25°C using a Sigma 700 surface tension meter (Sweden). Each measurement was repeated three times, and the average value was calculated. The data were plotted as a graph of surface tension (γ-mN/m) versus the logarithm of concentration (lgC) to determine the critical micelle concentration (CMC) of FNC.

2.3.4. FNC Surface tension measurement

To evaluate the salt tolerance of FNC, mineralized water solutions of $CaCl_2$ at concentrations of 5×10^3 mg/L, 1×10^4 mg/L, and 3×10^4 mg/L and NaCl (5×10^3 mg/L, 2×10^4 mg/L, 4×10^4 mg/L, and 8×10^4 mg/L) were prepared using deionized water. Subsequently, varying amounts of FNC were weighed and added to these mineralized water solutions to achieve different FNC concentrations (0.01%, 0.02%, 0.03%, 0.04%, 0.05%, 0.06%, 0.07%, 0.08%, 0.09%, 0.1%, 0.2%, and 0.3%), each corresponding to distinct salinity levels. Surface tension was measured at 25°C using a Sigma 700 surface tension meter (Sweden). Each test was conducted in triplicate, and the average values were calculated. Finally, surface tension curves for FNC under varying concentration and salinity conditions were plotted.

2.3.5. FNC Interfacial tension measurement

Deionized water was used to prepare mineralized water solutions containing $CaCl_2$ at concentrations of 5×10^3 mg/L, 1×10^4 mg/L, and 3×10^4 mg/L, and NaCl at concentrations of 5×10^3 mg/L, 2×10^4 mg/L, 4×10^4 mg/L, and 8×10^4 mg/L. Subsequently, varying masses of FNC were weighed and added to these mineralized water solutions to achieve FNC concentrations of 0.1%, 0.2%, and 0.3% under different mineralization levels. The interfacial tension between the FNC solutions and kerosene was measured at 25°C using a Sigma 700 interfacial tension meter. Three measurements were taken for each group, and the average value was calculated.

2.3.6. Contact angle measurement

Using the SDC-200S contact angle measuring instrument (Shengding Precision Instruments Co., Ltd.), the contact angles between FNC at different concentrations (0.1% and 0.2%) and a glass slide were measured in a 2×10^5 mg/L NaCl solution. All solutions were prepared with deionized water. Each test was repeated three times, and the average value was calculated.

3. Results and discussion

3.1 FTIR analysis

The FTIR spectra of FNA, FNB, and FNC are shown in Fig. 2. For FNA, the absorption peak at 3424 cm^{-1} corresponds to the N–H stretching vibration; the peak at 1633 cm^{-1} corresponds to the in-plane bending vibration of –NH; the peak at 1356 cm^{-1} corresponds to the asymmetric vibration of $–SO_2NH$; and the peak at 1190 cm^{-1} corresponds to the C–F stretching vibration, indicating that a sulfation reaction has occurred. For FNB, the absorption peak at 3416 cm^{-1} corresponds to the N–H stretching vibration; the peak at 1632 cm^{-1} corresponds to the in-plane bending vibration of –NH; and the peak at 1591 cm^{-1} corresponds to the C = C stretching vibration. This indicates that a quaternization reaction occurred between 5-chloro-1-pentene and FNA. For FNC, the absorption peak at 3422 cm^{-1} corresponds to the O–H stretching vibration; the peak at 3148 cm^{-1} corresponds to the = C–H stretching vibration; the peak at 1630 cm^{-1} corresponds to the C = O stretching vibration; and the peak at 1591 cm^{-1} corresponds to the C = C stretching vibration. These results indicate that 3-chloropropionic acid undergoes a nucleophilic substitution reaction with FNB.

3.2 ^{1}H-NMR and ^{19}F-NMR analysis

The ^{1}H-NMR spectrum of FNC is shown in Fig. 3. ^{1}H-NMR (400 MHz, ACETONITRILE-D3) δ 6.11 (m, 2H), $=CH_2$; 5.62 (dd, J = 9.5, 3.0 Hz, 1H), =CH; 3.54 (m, 2H), $N\text{-}CH_2\text{-}CO$; 3.41 (m, 2H), $N\text{-}CH_2$; 3.32–3.21 (m, 2H), $N\text{-}CH_2$; 3.00 (s, 6H), $N\text{-}CH_3$; 2.62 (m, 2H), $=C\text{-}CH_2$; 2.66–2.51 (m, 4H), $=C\text{-}CH_2$, $N\text{-}C\text{-}CH_2$; 2.04 (m, 2H), CH_2.

The ^{19}F-NMR spectrum of FNC is shown in Fig. 4. ^{19}F-NMR (500 MHz, D2O):δ:-82.2– -82.7 (3F, $\mathbf{CF_3}CF_2CF_2CF_2$-), δ: -112.6– -113.6(2F,$CF_3\mathbf{CF_2}CF_2CF_2$-), δ: -122.2(2F, $CF_3CF_2\mathbf{CF_2}CF_2$-),δ: -126.9– -127.2 (2F, $CF_3CF_2CF_2\mathbf{CF_2}$-).

3.3 CMC talue measurement

As shown in Fig. 5, the surface tension of the solution decreased significantly with increasing FNC concentration. Once the concentration reached a certain threshold, the surface tension stabilized. This behavior occurs because, at this point, FNC molecules have fully adsorbed at the gas–liquid interface, reaching saturation. This inflection point corresponds to an FNC critical micelle concentration (CMC) of 6×10^{-2} g/L.

3.4 Surface tension testing

As shown in Fig. 6, the experimental results indicate that in Fig. 6(a), at a constant $CaCl_2$ concentration, the surface tension decreases significantly as the FNC concentration increases. Conversely, as the $CaCl_2$ concentration increases, the surface tension of the FNC solution at the same concentration also increases, although this trend is not pronounced. However, when the FNC concentration reaches 0.3 wt%, the surface tension remains nearly constant at approximately 25.5 mN/m despite increasing $CaCl_2$ concentration. In Fig. 6(b), as the NaCl concentration increases, the surface tension of the solution decreases, reaching a minimum value of 21.62 mN/m at a NaCl concentration of 2×10^5 mg/L and an FNC concentration of 0.3 wt%. These results indicate that FNC not only exhibits strong surface activity but also demonstrates excellent salt tolerance.

3.5 Interfacial tension teasurement

As shown in Fig. 7, the interfacial tension decreases rapidly as the mass fraction of FNC increases. Figure 7(a) illustrates that the interfacial tension of the FNC solution continuously decreases with increasing NaCl concentration. When the NaCl concentration is below 2×10^4 mg/L, the interfacial tension of the FNC solution remains higher than that of the FNC solution in pure water; however, when the NaCl concentration exceeds 2×10^4 mg/L, and the FNC mass fraction exceeds 0.2%, the surface tension of the solution becomes lower than that of the FNC solution in pure water. Figure 7(b) shows that in $CaCl_2$ solutions, the interfacial tension of FNC in pure water is consistently lower than that in $CaCl_2$ solutions. However, when the $CaCl_2$ concentration exceeds 1×10^4 mg/L, the interfacial tension gradually decreases as the $CaCl_2$ concentration increases. These results indicate that FNC possesses excellent salt resistance.

3.6 Contact angle

The experimental results are presented in Table 1. At the same FNC concentration, as the degree of mineralization increases, the contact angle between the solution and the glass slide decreases, indicating that FNC exhibits good salt resistance.

Table 1
Contact Angle of FNC at Various NaCl Concentrations

Blank glass plate	**Contact angle (°)**		
	59.662	**58.555**	**58.535**
0.1% FNC Clear water	27.354	28.116	27.964
0.1% FNC (1 × 10^4 mg/L NaCl)	26.852	26.668	26.431
0.1% FNC (2 × 10^4 mg/L NaCl)	24.207	28.294	27.570
0.2% FNC Clear water	24.051	24.103	23.829
0.2% FNC (1 × 10^4 mg/L NaCl)	23.819	23.597	23.254
0.2% FNC (2 × 10^4 mg/L NaCl)	22.100	31.418	30.683

4. Conclusions

In this study, a novel perfluorobutylsulfonyl amphoteric surfactant (FNC) was synthesized, and its successful synthesis was confirmed through FTIR and NMR characterization. With a CMC value of 6 × 10^{-2} g/L, FNC exhibits excellent salt tolerance and surface activity, as demonstrated by surface tension, interfacial tension, and contact angle measurements. This work provides a valuable reference for the preparation and development of environmentally friendly, highly salt-tolerant fluorinated surfactants.

Declarations

The authors declare no competing financial interest.

Author Contribution

Z.H. Research Topics, Conducted experimental research, Analyzed data, and Drafted the manuscript. D.L.J. Confirmation of Research Topic, Data analysis, Data collection. L.B. Data analysis, Data collection. Y.X.Y. Review of experimental data, Revision of the paper L.X.J. Revision of the paper J.Z.F. Thesis review, data analysis, literature review, funding All authors reviewed the manuscript

References

1. YIN S, ZHANG L, WANG Y (2025) Role of Surfactant Emulsification Ability in Chemical Flooding and Advances in Enhanced Oil Recovery[J]. Journal of GeoEnergy, 2025: 2292980. https://doi.org/10.1155/jge5/2292980
2. YANG X, LIU H, ZHANG J (2024) Research progress on fracturing fluid system for deep coalbed methane reservoirs[J]. J Petrol Sci Eng 239:112965. https://doi.org/10.1016/j.petrol.2024.112965

3. HOU J, LI M, ZHAO Y (2025) Challenges of high salinity formation water on fracturing fluid surfactant performance in deep unconventional reservoirs[J]. Fuel 380:133126. https://doi.org/10.1016/j.fuel.2025.133126
4. SHARMA MK (2024) Limitations of conventional surfactants in high-salinity oil and gas reservoir development[J]. Colloids Surf A 685:133201. https://doi.org/10.1016/j.colsurfa.2024.133201
5. ABDURRAHMAN M, AHMAD SULAIMANS (2023) Research advances in salt-tolerant surfactants for oilfield development and reservoir stimulation[J]. ACS Omega 8(45):41004–41021. https://doi.org/10.1021/acsomega.3c04450
6. Cao B, Li L, Ma F (2025) Design and Evaluation of a Thermally Stable and Salt-Resistant Amphoteric Surfactant-Based Fracturing Fluid for High-Performance Hydraulic Stimulation[J]. Polymers 17(20):2741. https://doi.org/10.3390/polym17202741
7. Fan T, Lian Y, Zhao D et al (2026) Optimised synthesis of betaine surfactant for integrated air foam oil displacement and corrosion inhibition[J]. Corros Eng Sci Technol 61(3):360–372
8. Hou Z, Jiang W, Wu X et al (2026) Critical Review on the Molecular Behavior of Surfactants at the Oil–Water Interface During Oil Displacement[J]. Energy Science & Engineering
9. Karimov D, Imekova G, Toktarbay Z et al (2025) Experimental and numerical simulation studies of the zwitterionic polymers for enhanced oil recovery[J]. Sci Rep 15(1):34728
10. Peng W, You Q, Liu X et al (2025) Enhance oil recovery in fracture-cave carbonate reservoirs using zwitterion-anionic composite surfactant system[J]. Energies 18(2):383
11. Ghaleh Golab E (2025) Evaluation of zwitterionic and polymeric surfactant adsorption for enhanced oil recovery in sandstone reservoirs with high salinity conditions[J]. J Petroleum Explor Prod Technol 15(11):1–31
12. Kredel J, Gallei M (2020) Ozone-degradable fluoropolymers on textile surfaces for water and oil repellency[J]. ACS Appl Polym Mater 2(7):2867–2879
13. Sharma SC, Acharya DP, García-Roman M et al (2006) Phase behavior and surface tensions of amphiphilic fluorinated random copolymer aqueous solutions[J]. Colloids Surf A 280(1–3):140–145
14. Taylor CK (1999) Fluorinated surfactants in practice[J]. Annu Surfactants Rev 2:271–316
15. Chen C, Lu Y, Zhang X et al (2009) A review of spatial and temporal assessment of PFOS and PFOA contamination in China[J]. Chem Ecol 25(3):163–177
16. Liu Langlang L, Lun L (2009) Research Hotspots and Development Directions of Fluorinated Surfactants[J]. China Clean Ind 3:40–42
17. Giesy JP, Kannan K, Peer R et al (2002) Perfluorochemical surfactants in the environment[J], vol 36. Environmental Science & Technology, pp 146A–152A. 7

Figures

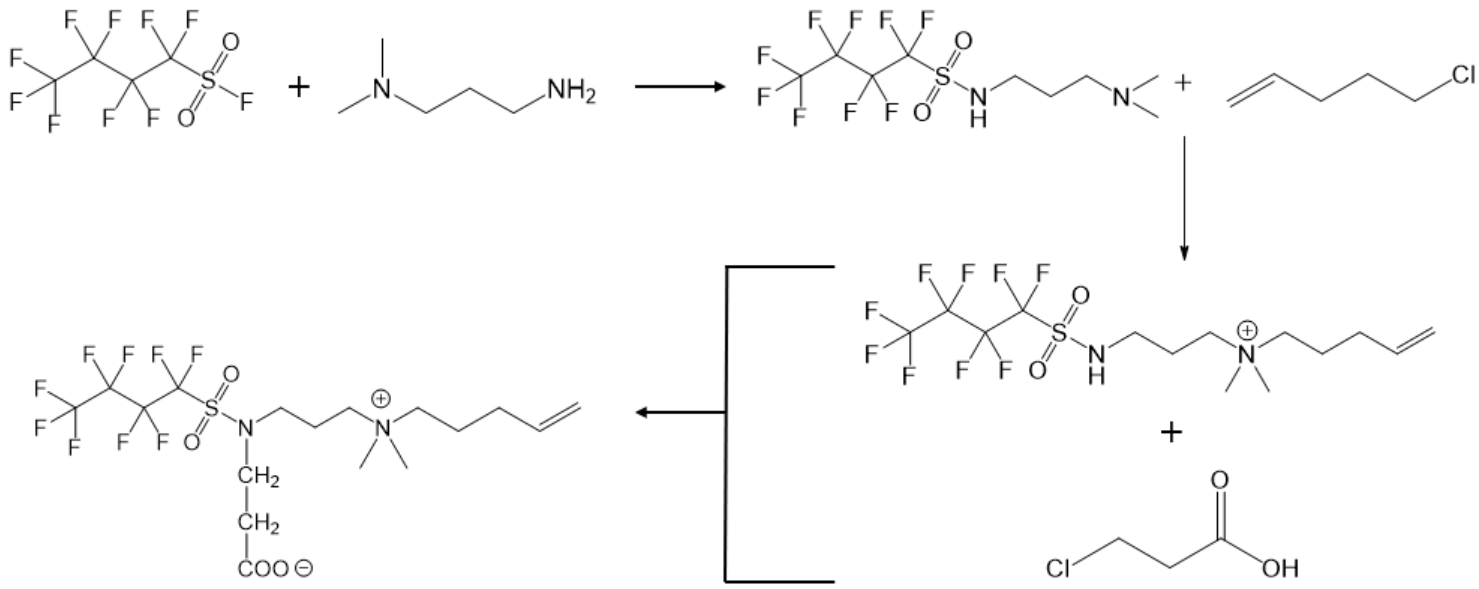


Figure 1

Synthetic route to FNC.

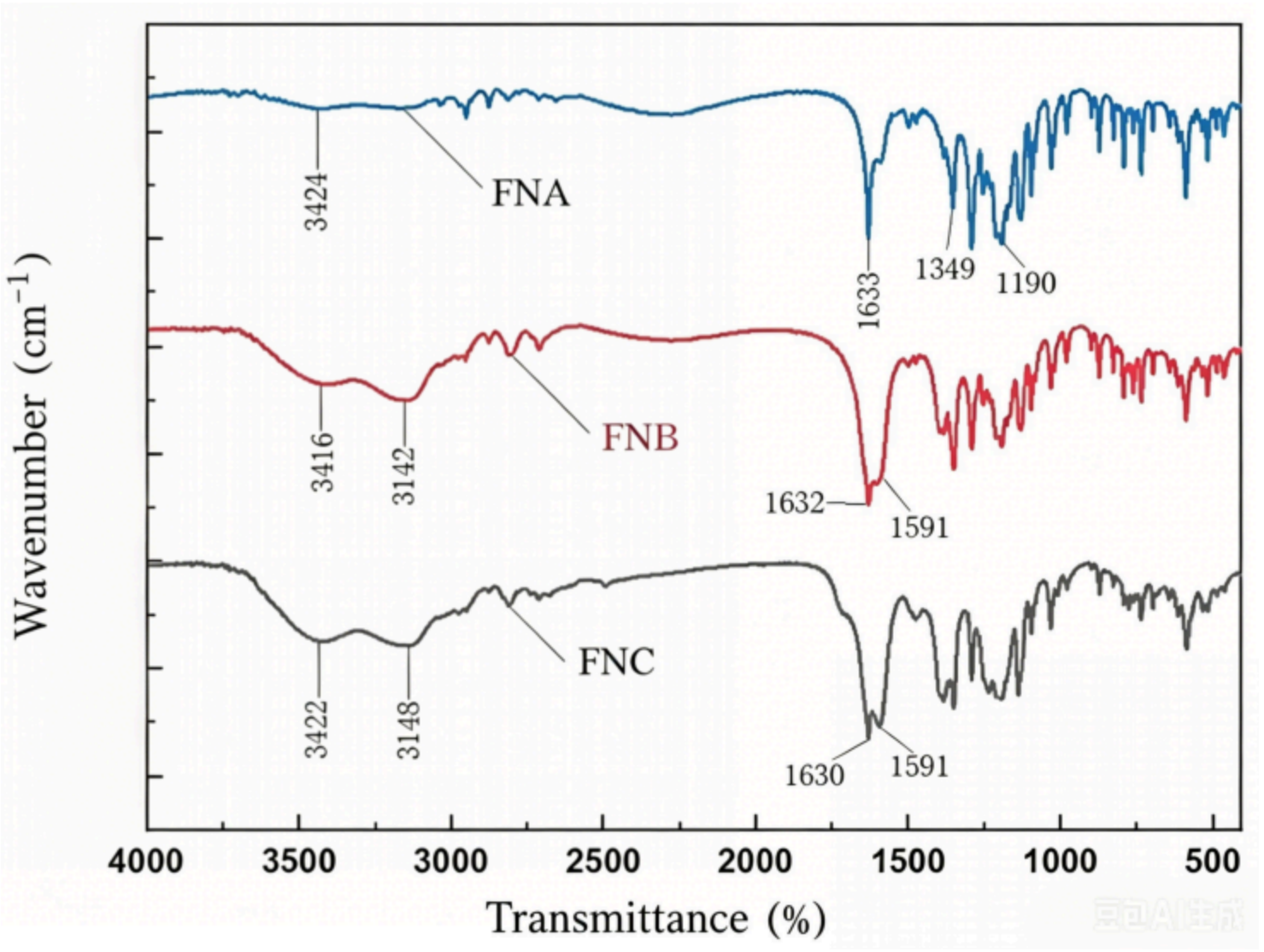


Figure 2

FTIR spectra of FNA, FNB, and FNC.

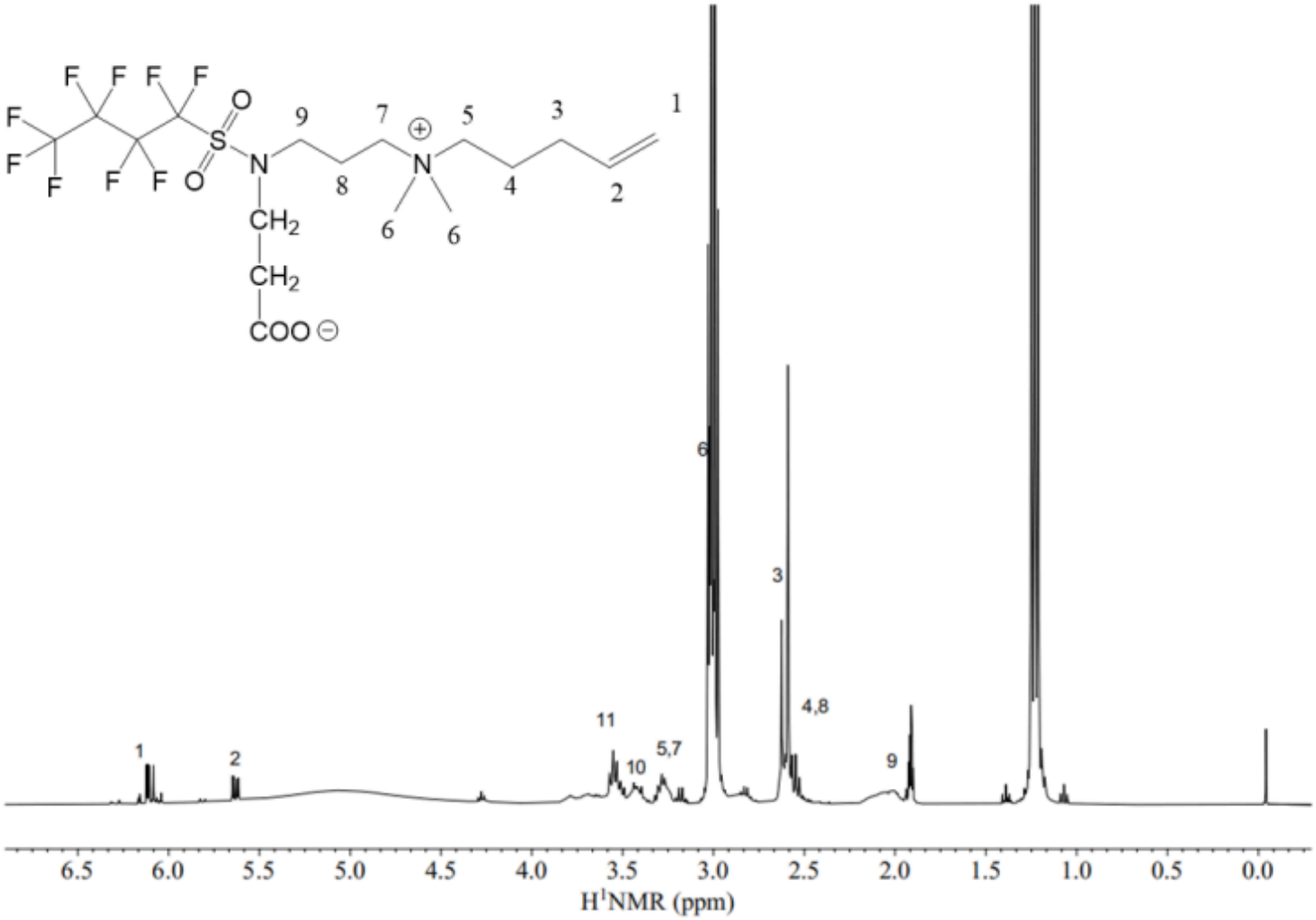


Figure 3

FNC ^{1}H-NMR Spectral Analysis

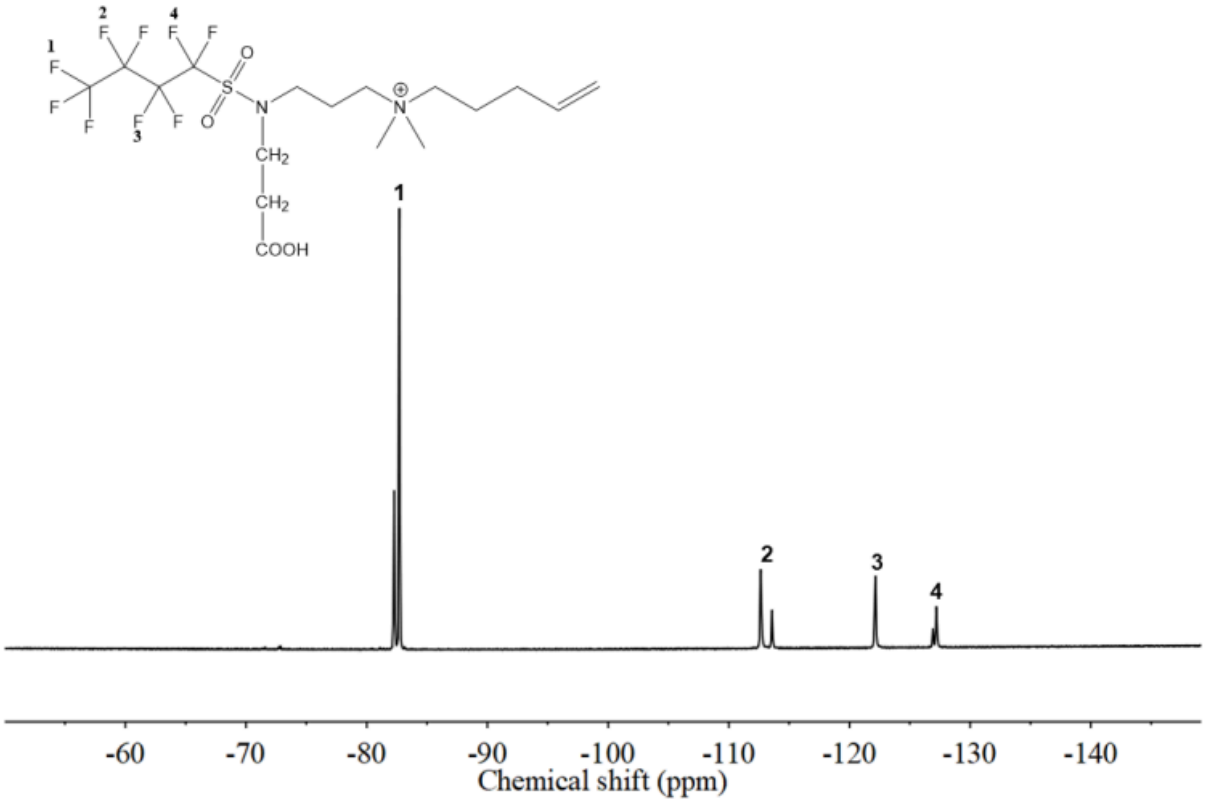


Figure 4

FNC ^{19}F-NMR Spectral Analysis

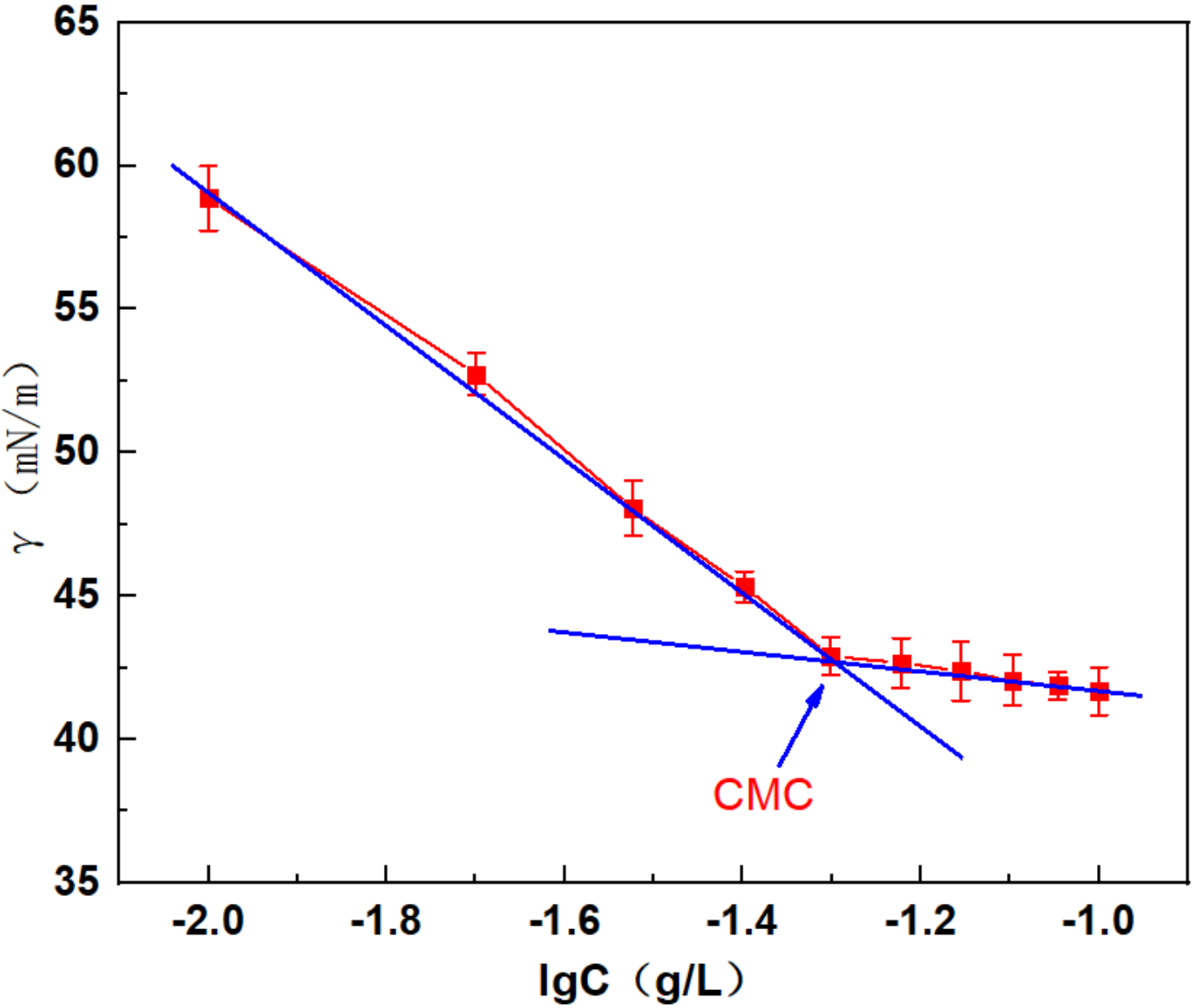


Figure 5

Determination of the Critical Micelle Concentration (CMC) of FNC

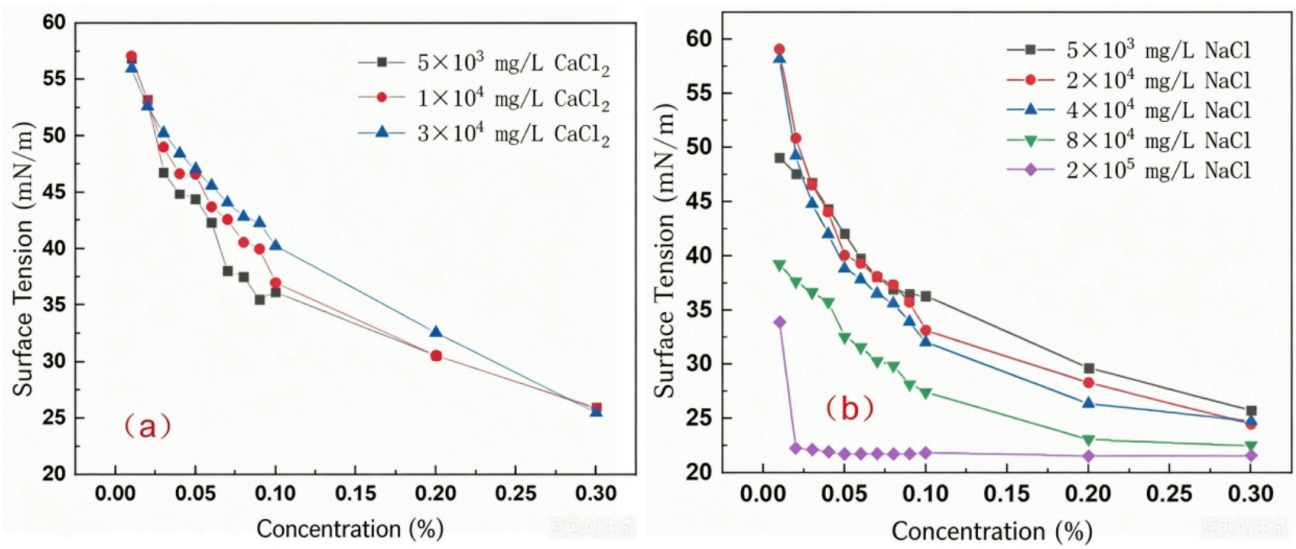


Figure 6

Surface Tension of FNC Solutions at Various Concentrations of $CaCl_2$ (a) and NaCl (b)

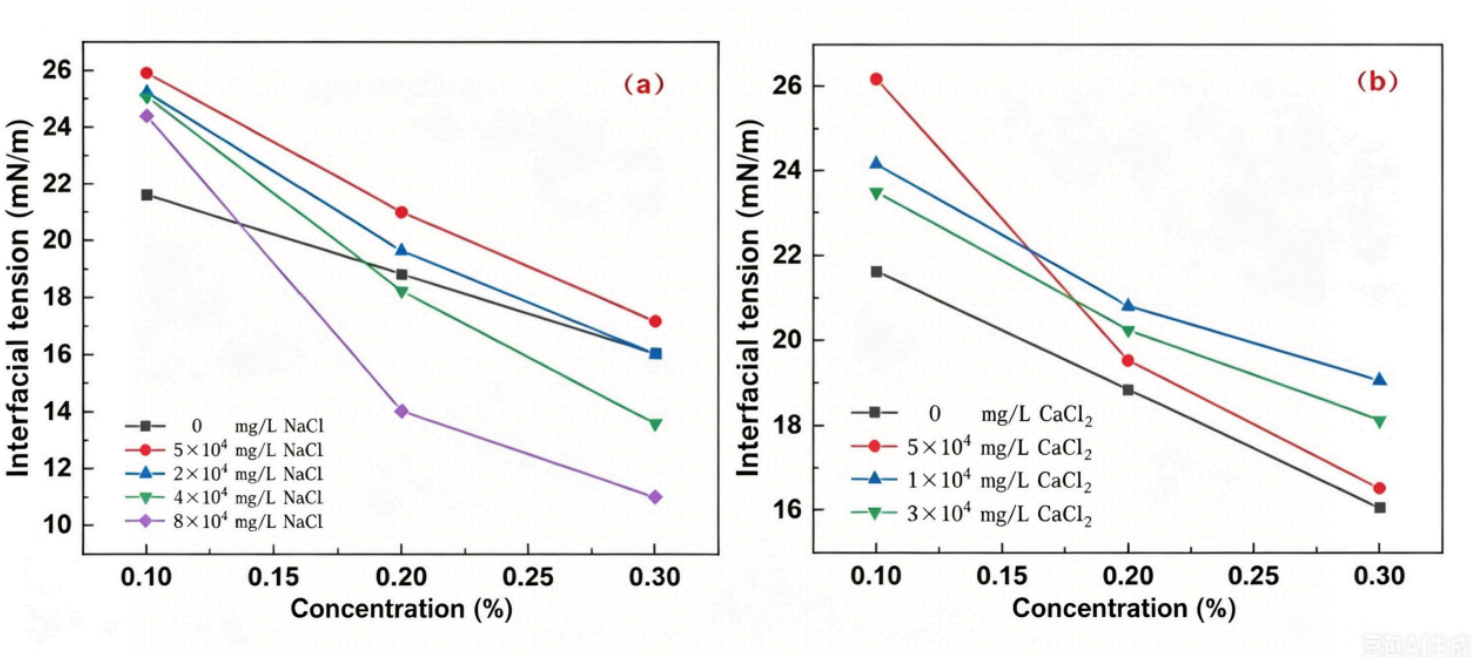


Figure 7

Interfacial Tension of FNC Solutions at Various Concentrations of NaCl (a) and $CaCl_2$ (b)